ELSEVIER

S0032-3861(96)00583-6

Polymer Vol. 38 No. 4, pp. 759–768, 1997

0032-3861/97/$17.00 + 0.00

A synchrotron X-ray study of melting and recrystallization in isotactic polypropylene*

Anthony J. Ryan†‡ and John L. Stanford
Manchester Materials Science Centre, UMIST, Grosvenor Street, Manchester M1 7HS, UK

and Wim Bras§
CLRC Daresbury Laboratory, Warrington WA4 4AD, UK

and Thomas M. W. Nye
Department of Applied Mathematics, Cambridge University, Cambridge CB3 9EW, UK
(Received 26 January 1996; revised 3 May 1996)

SAXS/WAXS/d.s.c. at the SRS has been used to follow the melting and recrystallization of isotactic polypropylene (iPP). The time correlation is perfect between the three techniques which show good agreement with respect to crystallinity and kinetics. The degree of crystallinity and the lamellar thickness of iPP have been calculated from SAXS and WAXS patterns, obtained simultaneously during melting and crystallization, by integrated intensity and correlation function techniques. The long spacing was obtained from the peak in the Lorentz-corrected SAXS pattern and was in good agreement with that calculated from the correlation fuction (γ_1). The degree of crystallinity was obtained from a combination of the SAXS invariant and the integrated WAXS intensity (due to the crystals), and the local crystallinity was obtained from γ_1. The data obtained during melting and recrystallization were interpreted in terms of a polydisperse lamellar model.

(Keywords: polypropylene; X-ray scattering; correlation function)

INTRODUCTION

The crystal structure and crystallization kinetics of isotactic polypropylene are well established[1]. The monoclinic (space group $P2_1/c$) unit cell and the lamellar arrangement of crystalline and amorphous regions into fibrils and spherulites are also well known[1]. *Figure 1* illustrates the heirarchical nature of polymer spherulites on a scale ranging from mm down to Å. The degree of crystallinity, defined as either the weight or the volume fraction of the crystalline phase, is of fundamental importance in defining the physical and chemical properties of a semi-crystalline polymer as demonstrated, for example, in a recent study[2] in which the relationship was established between the mechanical properties, the degree of crystallinity and the lamellar thickness in polypropylene films.

The importance of producing accurate and reproducible data, that is the degree of crystallinity and lamellar thickness, in order to model the mechanical properties of iPP, is readily apparent. Several methods are used[3] to evaluate the degree of crystallinity and include density (density column), calorimetry (d.s.c. and d.t.a.), spectroscopy (n.m.r., *FT*i.r., and Raman) and X-ray techniques such as wide- and small-angle scattering (WAXS and SAXS). Each of these methods is based on a different physical feature and uses a different definition of crystalline order. Furthermore, measurements of the degree of crystallinity and lamellar thickness do not give equilibrium values since these properties are associated with metastable states of a semi-crystalline polymer that are dependent on thermal history. Such factors explain the different values for these properties, obtained using the various methods, reported in the literature (see for example the 'Polymer Handbook'[4]). Some of these methods rely inevitably on a calibration involving wholly-crystalline and/or wholly-amorphous standards and, furthermore, they are limited generally to making single-point measurements on stable systems: this is especially true of the density column technique. Lamellar thickness is intrinsically more difficult to obtain quantitatively. Three main methods are used: (i) transmission electron microscopy[5] where the direct image of lamellae is analysed; (ii) WAXS where either the shape of the Debye–Scherer peak is analysed for mosaicity[6] or the whole-pattern curve-fitting technique of Ruland[7] is analysed; and (iii) SAXS where either the long-spacing from the peak position is multiplied by the degree of crystallinity obtained from another technique[8], or the correlation function is used[9–11] with the linear crystallinity being determined by the ratio of the long period and the lamellar thickness.

Crystallization kinetics are also of technical

* This paper is dedicated to the memory of Professor H. G. Zachmann, a pioneer of the application of synchrotron radiation to the study of polymers

† To whom correspondence should be addressed

‡ Also at CLRC Daresbury Laboratory, Warrington WA4 4AD, UK

§ Also at AMOLF, Kruislaan 407, 1098 SJ, Amsterdam, The Netherlands

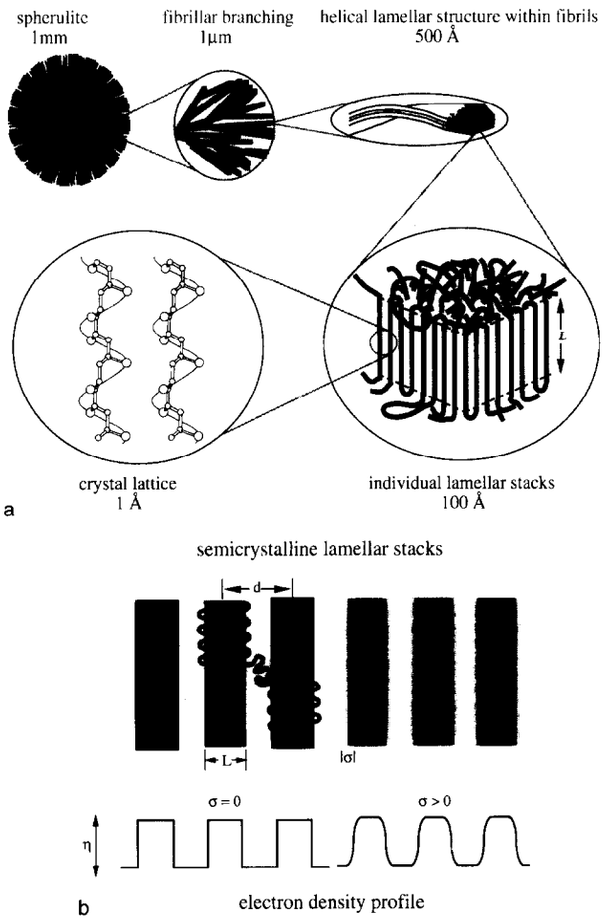

Figure 1 (a) A schematic representation of the hierarchal structure of polymer crystals ranging from the mm (spherulite) to the Å scale (repeat units in extended polymer chains). (b) A simple two-phase SAXS model for polymer crystals[9], illustrating both sharp interfaces ($\sigma = 0$) and sigmoidal interfaces ($\sigma > 0$)

importance[1,3] in terms of solidification rates used during processing by moulding or extrusion. The earliest reported methods for studying kinetics of crystallization are measurements of volume change. In order to study crystallization kinetics by this technique, an isothermal bath is essential as the only change in volume must be that associated with the crystallization process: the volume change data obtained are interpreted in terms of an Avrami model[12]. Isothermal d.s.c. is an alternative method of studying crystallization kinetics involving measurement of the enthalpy of crystallization[1]. Both of these techniques have reasonable time-resolutions (< 1 s with automation) but are limited to isothermal studies. The d.s.c. technique can be used for non-isothermal crystallization but analysis of d.s.c. data obtained involves many assumptions and is both model dependent and computationally intense[13]. The limitation of volume and enthalpy techniques is that they only access the overall rates of crystallization in terms of nucleation and growth.

The radial growth rate of polymer spherulites may be studied, independently of nucleation, using optical microscopy[14]. Unlike the overall rate of crystallization, which is dominated by the nucleation process, the radial growth rate, ν, is a function only of the degree of undercooling and molar mass for a given polymer. Within spherulites, the commonest form of melt-crystallized polymer, the polymer chain axes are perpendicular to the spherulite radius. Thus the growth phenomenon is simplified in one-dimensional terms, so that the lateral growth is generally observed to be linear with time. The growth process is a property of the polymer and is dependent on supercooling, molar mass, molecular architecture (branching) and tacticity but *not* on the nucleation mechanism, and ν passes through a maximum between T_g and T_m. The temperature dependence of ν is qualitatively interpreted as the complex product of the driving force for crystallization and the molecular mobility of the system. As the temperature is reduced from the thermodynamic melting point, T_m^0, the driving force for crystallization, ϵ, increases as it is directly proportional to the under-cooling, given as $\epsilon \sim (T_m^0 - T)$. The mobility of the system decreases asymptotically as the glass transition temperature is approached since molecular mobility is reciprocally related to the viscosity, by $\eta \sim 1/(T - T_g)$. The optical microscopy technique, therefore, is very useful for observing the isothermal growth process and, at best, has a time resolution ($\sim$ 40 ms) associated typically with video techniques.

Time-resolved X-ray scattering techniques, using synchrotron radiation, give the option of obtaining, *simultaneously*, the crystallization rate and the crystal size. The objective of this work is to identify reliable methods of obtaining crystallization kinetics and crystal thicknesses for on-going research in polymer processing. There have been a relatively small number of studies on iPP and other polyolefins using time-resolved SAXS and WAXS. The melting behaviour of LDPE has been studied by time-resolved SAXS[15] and the correlation function used to extract the data for lamellar thickening. The novel technique of simultaneous SAXS/WAXS has been used to study polymorphism in iPP, and the various crystal forms that exist[1], depending on cooling cycles and the transformation from the quenched (smectic) structure to the monoclinic crystal on heating, have been investigated[16]. Analysis of the invariant and of the integrated WAXS intensities showed that the transformation was continuous with an onset temperature of $\approx 60°C$. The wide-angle scattering gave quantative information on the crystal structure and the invariant allowed the relative proportions of the two crystal structures to be calculated.

This paper demonstrates the effectiveness of using simultaneous SAXS/WAXS/d.s.c. to study the crystallization kinetics and the development of crystal structure of an unfilled, semicrystalline polymer. The results show how the combination of integrated intensities (SAXS invariant and WAXS peaks) and SAXS correlation functions allows unambiguous determination of the volume fraction of crystals, volume fraction of spherulites, the intralamellar degree of crystallinity and the lamellar thickness during the crystallization process.

EXPERIMENTAL

Materials

The polypropylene used was a commercial grade, S-30-S (ex. Himont) which was free from any additives. The number-average molar mass (g.p.c.) and the polydispersity were, respectively, 62.2 kg mol^{-1} and

5.89[17], and the melting point (d.s.c.) was $170 \pm 2°C$[18]. The as-received iPP pellets had a degree of crystallinity of 0.6 as determined from measurements of the heat of fusion.

SAXS/WAXS/d.s.c.

Simultaneous SAXS/WAXS/d.s.c. measurements were made on beamline 8.2 of the SRS at the SERC Daresbury Laboratory, Warrington, UK. The details of the storage ring, radiation and camera geometry and data collection electronics have been given in detail elsewhere[19]. The camera is equipped with a multiwire quadrant detector (SAXS) located 3.5 m from the sample position and a curved knife-edge detector (WAXS) that covers 120° of arc at a radius of 0.2 m. A vacuum chamber is placed between the sample and detectors in order to reduce air scattering and absorption. The exit window of the beam-line and the entrance window of the vacuum chamber are both made from mica (thickness 75 μm): the exit windows of the vacuum chambers for the WAXS and SAXS detectors are made, respectively, from Mylar (thickness 150 μm) and Kapton film (thickness 50 μm). The WAXS detector has a spatial resolution of 100 μm and can monitor up to $\sim$ 50 000 counts s^{-1}; only 60° of arc are active in these experiments with the rest of the detector being shielded with lead. A beamstop is mounted just before the SAXS exit window to prevent the direct beam from hitting the SAXS detector which measures intensity in the radial direction (over an opening angle of 70° and an active length of 0.2 m) and is suitable only for isomorphous scatterers. The spatial resolution of the SAXS detector is 400 μm and it can handle up to $\sim$ 500 000 counts s^{-1}.

Disk specimens of iPP (thickness $\sim$ 1 mm, diameter $\sim$ 8 mm) were cut from pre-moulded sheet. A disk specimen for SAXS/WAXS/d.s.c. was encapsulated in a TA Instruments d.s.c. pan fitted with mica windows (thickness $\sim$ 25 μm, diameter $\sim$ 7 mm)[20], and the pan was inserted into a Linkam d.s.c. apparatus of the single-pan design that has been described in detail elsewhere[21,22]. The cell comprises a silver furnace around a heat-flux plate containing a 3×0.5 mm slot, for X-ray access, and the sample is held in contact with the plate by a spring of low thermal-mass. A reference (calibration) sample of the same thermal mass was first subjected to the temperature ramp and the thermal response of the neutral system was recorded. The iPP sample was then run and its thermal response recorded, and the differential response was subsequently calculated from the electronic recordings. The single-pan technique relies on the accuracy and reproducibility of the temperature control system, and produces data comparable to those of a conventional two-pan, heat-flux d.s.c. such as, for example, a TA Instruments 990 apparatus[22].

In the present study, a three-stage temperature programme was used as follows: (i) heat from 100 to 200°C at 20°C min^{-1}; (ii) hold at 200°C for 1 min; (iii) cool at 60°C min min^{-1} to the crystallization temperature of 133°C and hold for $\sim$ 17 min. The crystallization temperature was chosen so that the primary crystallization kinetics were obtainable within a reasonable ($\sim$ 17 min) time-scale, and the crystals formed were primarily α-spherulites of the monoclinic form.

The scattering pattern from an oriented specimen of wet collagen (rat-tail tendon) was used to calibrate the SAXS detector and HDPE, aluminium and an NBS silicon standard were used to calibrate the WAXS detector[16,21,22]. Parallel-plate ionization detectors, placed before and after the sample cell, recorded the incident and transmitted intensities. The experimental data were corrected for background scattering (by subtracting the scattering from the camera, the hot-stage and the empty cell), for sample thickness and transmission, and for the positional alinearity of the detectors.

The data acquisition systems for SAXS/WAXS and d.s.c. comprise separate computers. The PC-based controller for the d.s.c. was used to initiate the SAXS/WAXS data collection once the first control temperature was reached. The beam-line data acquisition system has a time-frame generator which collects the SAXS/WAXS data in 6 s-frames separated by a wait-time of 10 μs and during the wait-time, a high-voltage pulse was written over the d.s.c. signal in order to give perfect time correlation between the SAXS/WAXS and d.s.c. data[21,22].

Data analysis

The important features of the WAXS and SAXS patterns and the quantities derived from them are shown schematically in *Figure 2*. The data analysis is restricted to primary crystallization and the reader is referred to a review of secondary crystallization by Zachmann *et al.*[23].

The peaks in a one-dimensional WAXS pattern of a randomly-oriented polycrystalline material may be indexed to the crystal structure. Furthermore for a semi-crystalline material, the degree of crystallinity may be calculated from the pattern, and there are two comparative methods applicable to the determination of the degree of crystallinity by WAXS[6,24]. External

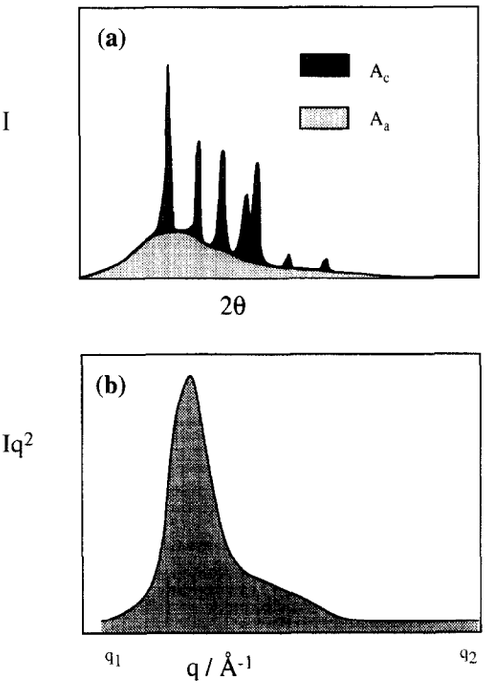

Figure 2 Generalized X-ray scattering curves. (a) WAXS curve showing crystalline peaks with the integrated intensities (represented by the dark-shaded areas) used to determine A_c, and an integrated amorphous halo (light-shaded area) used to determine A_a. (b) SAXS curve in which the shaded area represents the relative invariant, Q', evaluated according to equation (2)

methods involve comparison of an experimental WAXS pattern of a semi-crystalline material to those of wholly-crystalline and wholly-amorphous standards of the same material. Internal methods use the integrated intensities of the pattern associated with the amorphous and crystalline features that actually form the semi-crystalline material. To a first approximation, the degree of crystallinity can be obtained by assuming that the total scattering within a certain region of reciprocal space is independent of the state of aggregation of the material. The degree of crystallinity, X_c expressed as the mass fraction of crystalline component, is then given as

$$X_c = A_c/(A_c + A_a) \quad (1)$$

where A_a is the area under the amorphous halo and A_c is the area remaining under the crystalline peaks as shown, for example, by the simplified schematic diagram in *Figure 2*. A simple integration for WAXS is used because the peak line-shape is somewhat limited by instrument resolution and as such, any curve-fitting routine will be a convolute of both the instrument resolution and the intensity. The integrated intensity over the four main peaks gives the value of A_c and the integrated intensity over adjacent areas without peaks gives the value of A_a, allowing $A_t (= A_c + A_a)$ to be calculated after normalization for pixel size. Without either numerical analysis of the whole pattern or in the absence of any method of calibration, the integrated intensities of strong reflections give values of X_c with a precision of ±7%, and therefore provide only semi-quantitative information on the degree of crystallinity. The magnitudes of A_c, A_a, and A_t, when $X_c = 0$ (that is, when $T \gg T_m$) and X_c is a maximum, are known. Furthermore, there is an external calibration (during melting) at $X_c = 0$ and at $X_c = 0.5$.

Information regarding microstructural periodicity may be obtained from unoriented SAXS patterns provided the morphology is assumed to be globally isotropic but locally lamellar[6,7,9–11,23,24]. The data can then be analysed to give a one-dimensional Bragg spacing, d_1, by applying the Lorentz correction, q^2, to the observed scattering intensity, $I(q)$. If the first-order reflection is very strong and, additionally, if a second-order reflection is observed, then the interface between crystalline and amorphous regions is sharp and application of a two-phase model is appropriate. For the calculation of the Bragg spacing, the maximum in a plot of $I(q)q^2$ vs q is taken as q^*, so that $d_1 = 2\pi/q^*$.

The scattering power (also known as the invariant (Q)) may be obtained from the integral in equation (2). The absolute invariant may be used to calculate the degree of crystallinity and the lamellar thickness[6]. Determination of the absolute value of Q, however, requires absolute intensity measurements, subtraction of thermal background and extrapolation of $I(q)q^2$ vs q data to $q = 0$ and $q = \infty$. The major contribution to the experimental invariant can be used to characterize structure development and is readily obtained from integration of the $I(q)q^2$ vs q curve between more experimentally-accessible limits[25]. Hence, values of the relative invariant, Q', may be calculated by summation of the area under the $I(q)q^2$ vs q curve between the limits $q = q_1$, given as the first reliable data point, and $q = q_2$, taken from the region of the curve over which $I(q)q^2$ becomes constant. In the present analysis, the values of q_1, and q_2, chosen were 0.007 and 0.20 Å^{-1}, respectively.

$$Q' = \int_{0.007}^{0.200} (I(q) - I_b)q^2 \quad (2)$$

Due to the relative nature of the intensity measurement, the value of Q' is also only relative with arbitrary units. The truncation of the integral for the relative invariant has no significant effect on the derivative of the invariant with respect to temperature, and thus the relative invariant is used throughout the present study.

For the results presented in this paper, the processes of interest are melting and primary crystallization. The WAXS data maybe analysed to give X_c during both processes, whereas the derived SAXS data (giving values of the relative invariant, Q') is a complex function of structure and density and must be analysed differently during the processes as the data are dominated by different terms[23]. The invariant, Q, is a linear function of the square of the electron density difference, $\langle\eta^2\rangle$, between the crystalline and amorphous phases, and of the volume fraction of crystallites, and a quadratic function of the volume fraction of crystals in the lamellar stack and is given by

$$Q' = KS_S X_L(1 - X_L)\Delta\eta^2 \quad (3)$$

where K is a constant related to the scattering volume and the experimental equipment characteristics, X_S is the volume fraction of spherulites, X_L is the degree of crystallinity within the lamellar stacks and $\Delta\eta^2$ is the square of the electron density difference between the crystalline and amorphous polymer. The crystallinity measured by WAXS is given by the product $X_S X_L$ $(= X_C)$: for a well-crystallized material $X_S \rightarrow 1$ and, initially, $X_L = X_{Lmax}$ so that Q', is dominated, therefore, by the term $X_L(1 - X_L)$ and is sensitive to changes in X_L. Furthermore, $X_L(1 - X_L)$ passes through a maximum at $X_L = 0.5$. In a polymer melt, $X_S = X_L = 0$, and on primary isothermal-crystallization, $X_S \rightarrow 1$ with the value of $X_L = X_L^*$, where X_L^* is determined by the degree of under-cooling and the nucleation mechanism. Thus, during the melting process, X_S is a constant and Q' is a quadratic function of the degree of crystallinity whereas during crystallization, X_L is a constant and Q' is a linear function of the degree of crystallinity.

The SAXS data have also been analysed using a one-dimensional correlation function in terms of an ideal lamellar morphology[9–11]. The correlation function, designated γ_1, is essentially a Fourier transform of a given one-dimensional SAXS curve[9–11], and is often interpreted in terms of an imaginary rod moving through the structure of the material from which the SAXS curve was obtained, so that $\gamma_1(r)$ may be considered as the probability that the rod is of length, r, with equal electron densities at either end. Hence, a frequently-occurring spacing within a structure is manifested as a peak in the one-dimensional correlation function. The interpretation of $\gamma_1(r)$ assumes, that, within the SAXS length scale, spacings occur along one fixed axis, but that the axis assumes all possible directions throughout the material.

The task of calculating and interpreting the correlation functions can be summarized in three logical stages. The first involves extrapolation of the experimental SAXS curve to the limits of $q = 0$ and $q = \infty$ which is required mathematically in order to apply the Fourier transform. Any SAXS experiment gives only a finite number of intensity values at finite values of q, thus necessitating

this extrapolation and a numerical integration to calculate the transforms. Extrapolation to $q = \infty$ (referred to as tail-fitting) is the most problematic task of correlation function analysis and can greatly influence the results obtained. Care was taken not to introduce artefacts into the correlation function by truncation and joining errors. In the present study, the tail-fitting to $q = \infty$ was carried out using a damped Porod function of the form given by equation (4), in which the parameter σ characterizes the form of the interface,

$$I(q) = I_b + K e^{\sigma^2 q^2}/q^4 \quad (4)$$

and the forward extrapolation to $q = 0$ has been made according to Guinier's law. The second stage involves Fourier transformation of the extrapolated data to give $\gamma_1(r)$, which is based on a cosine Fourier transform of the form,

$$\gamma_1(r) = \frac{1}{Q}\int_0^\infty I(q)q^2 \cos(qr)\,dq \quad (5)$$

where Q is the extrapolated invariant described above and is used to normalize the transform so that $\gamma_1(0) = 1$. Thirdly, the correlation function, $\gamma_1(r)$, is interpreted on the basis of an ideal lamellar morphology[10] to yield the long spacing (L_p or d_γ), the lamellar thickness (L_γ), the interfacial thickness (D_{tr}) and the local degree of crystallinity (X_γ) from the ratio L_γ/d_γ.

RESULTS AND DISCUSSION

The SAXS and WAXS data, obtained during melting and crystallization of the iPP, are illustrated as three-dimensional plots and corresponding contour plots in *Figure 3*. Plots of the Lorentz-corrected SAXS intensity $I(q, t)q^2$ and the WAXS $I(2\theta, t)$ intensity vs $q(2\theta)$ vs t are shown in *Figures 3a* and *c*, respectively: the corresponding intensity contours are given in *Figures 3b* and *d*, respectively. In each case the time axis has been labelled in terms of temperature, and each diffraction pattern is a 6-s average during the temperature ramp and only every fourth pattern is shown for clarity. The three-dimensional WAXS data show most clearly the melting and recrystallization processes that occur from the variations in the intensities of the sharp *110*, *040*, *130*, (*111*, *131*, *041*) reflections of the monoclinic iPP crystals. During melting, the intensities decrease and melting of the material is continuous from the time at which measurements commenced ($\sim 100°C$) to the time at which the temperature reached $\sim 165°C$ ($= T_m$). (Temperatures are uncorrected from the Linkam d.s.c. and are, therefore, only approximate.) During crystallization, all the WAXS reflections develop concurrently as the material crystallizes.

The SAXS data illustate the morphological complexity of the melting and crystallization processes. The iPP sample has a totally spherulitic morphology that has developed under pressure at 128°C, and the sample has been slowly cooled so that, during the cooling process, secondary crystallization occurs increasing the degree of crystallinity[26]. During melting, the SAXS intensity increases during the temperature interval 100 to 160°C, and the peak position moves to lower values of q^*, that is, larger long-spacings which are easily observed in the SAXS contour plot. The phenomenon accounting for this change in q^* during melting is the initial melting of thin crystals which are formed during the fractionation processes that occurred during the previous crystallization. When a polymer recrystallizes, the degree of under-cooling is characterized by a value of lamellar thickness, L, determined according to the relation

$$L \propto K/(T_m^0 - T_C) \quad (6)$$

where K is a composite factor containing the heat of fusion and the fold surface energy. As the isothermal crystallization process occurs, via radial growth of spherulites comprising lamellae stacks, the peak position does not change as the SAXS comes only from intra-spherulite scattering.

The SAXS invariant and the integrated intensities from the WAXS are plotted against time in *Figure 4*.

In the temperature interval 100 to 200°C, that is the first 50 frames (where each frame is of 6 s duration), the WAXS intensities decrease continuously from a maximum value to a constant minimum value consistent with X_C falling from X_C^{max} to $X_C = 0$. (Off-line d.s.c. experiments showed the as-moulded polypropylene to be $\approx 70\%$ crystalline). Initially, as the material is heated, the SAXS invariant increases and according to equation (3), since $X_S = 1$, the term $X_L(1 - X_L)$ dominates Q' as local melting of thin lamellae occurs within spherulites. The peak in Q' is associated with $X_L = 0.5$ and, after correction for the difference in thermal expansivities between the amorphous and crystalline regions[23], the peak is used to calibrate the integrated WAXS intensities in terms of X_C, as described in a previous publication[24]. Eventually the spherulites melt and both X_L and X_S decrease to zero. During recrystallization, the SAXS invariant and the integrated WAXS intensities map directly onto each other, as $X_C = X_S X_L$. The lamellar thickness and degree of crystallinity within a lamellar stack are determined by the degree of under-cooling, with L and X_L remaining constant during primary crystallization and, as the spherulites grow, $X_S \to 1$.

The correlations between the SAXS, WAXS and d.s.c. data are illustrated in *Figure 5* where the derivatives, with respect to time (approximately equivalent to temperature), of the invariant and the degree of crystallinity are compared with the d.s.c. curve (which is the derivative with respect to temperature of the apparent heat capacity). The peak-to-peak correlation of the d.s.c. dQ/dt and dX/dt vs t curves indicate that the melting point may be determined to within one frame which, in terms of temperature, corresponds to $\pm 1°C$.

Asssuming the material may be described by a two-phase model[9-11] and correcting for the change in $\Delta\eta^2$ with temperature, then the invariant passes through a maximum at $\phi = 0.5$[23,24]. This assumption allows two further important procedures to be carried out. Firstly, the value of A_C when Q' is a maximum (I_{Q^*}) may be interpreted as being that at which the volume fraction of crystals $\phi = 0.5$. The relationship between volume and mass fractions of crystals is given by the simple expression

$$X_C = \phi\rho_c/\rho \quad (7)$$

where ρ_c is the density of pure crystal and ρ is the density of the semi-crystalline polymer. Thus, two points on the linear scale, $X_C = \phi\rho_c/\rho$, are known at $\phi = 0$ and $\phi = 0.5$, assuming that the density values of the semi-crystalline polymer vary linearly between the limits of

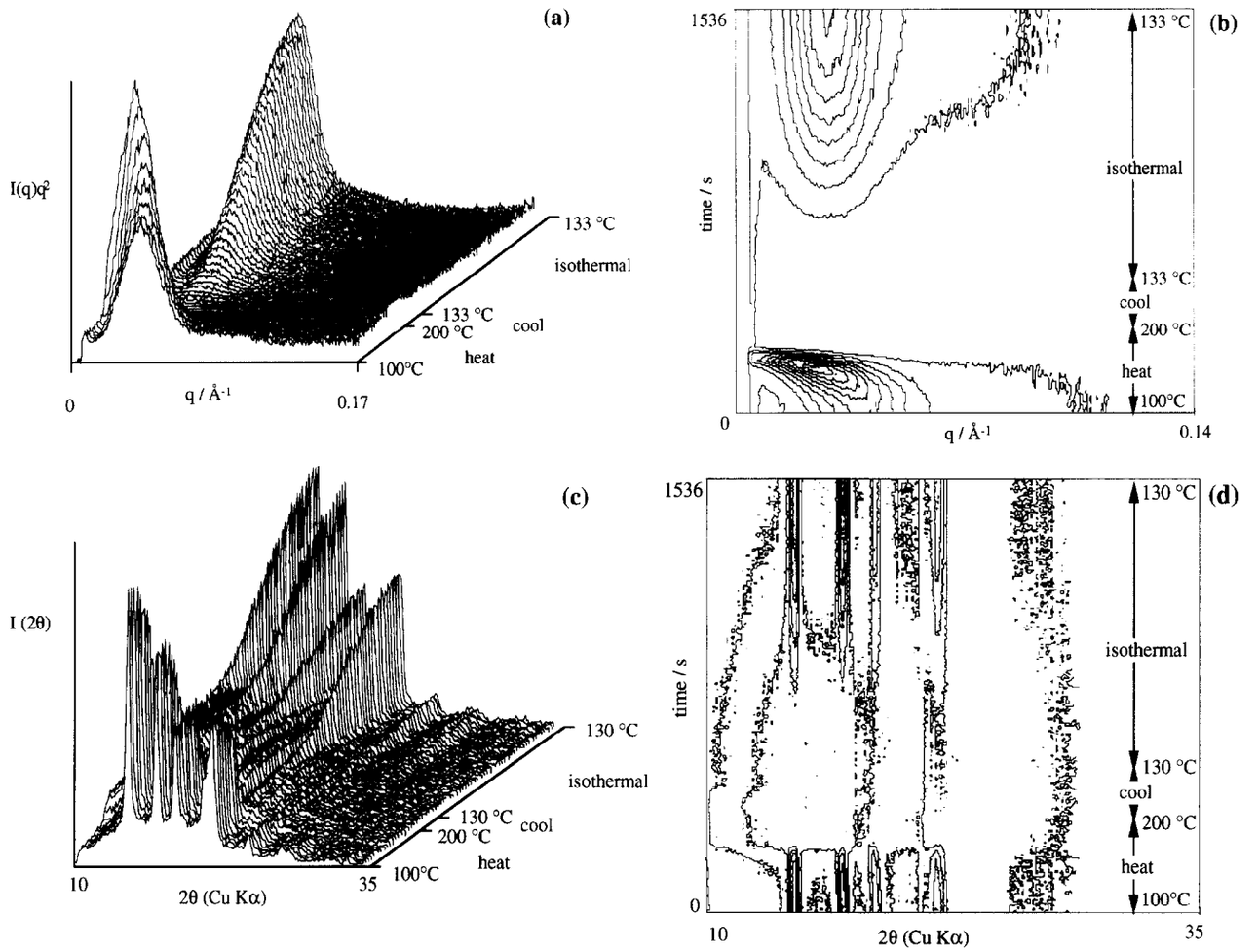

Figure 3 Three-dimensional relief diagrams and the corresponding contour plots of time resolved SAXS and WAXS data obtained with a time resolution of 6 s during the melting and recrystallization of iPP. For ease of interpretation, only every fourth pattern is shown. (a) Three-dimensional plot of Lorentz-corrected SAXS intensity, $I(q,t)q^2$ vs scattering vector q vs temperature T. (b) SAXS contour plots with intensity contours in the Lorentz-corrected intensity, $I(q,t)q^2$ vs scattering vector q vs time t. The inset gives the corresponding thermal cycle. (c) Three-dimensional plot of WAXS intensity, $I(2\theta,t)$ vs scattering vector q vs temperature T. (d) WAXS contour plots with intensity contours in the scattered intensity, $I(2\theta,t)$, *versus* the scattering angle 2θ vs time t. The inset gives the corresponding thermal cycle

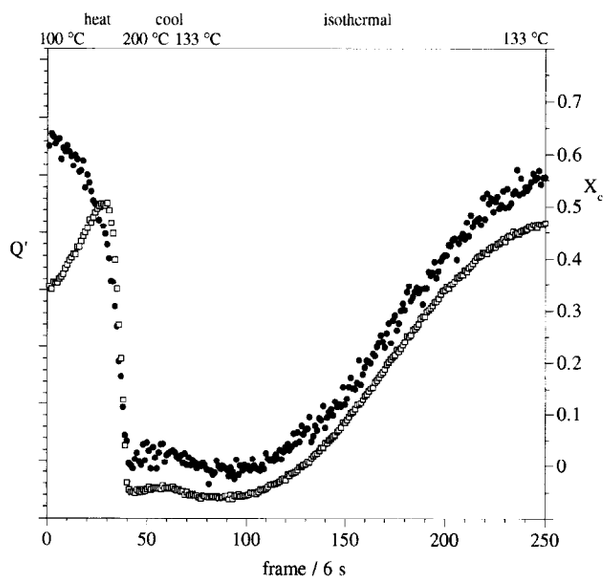

Figure 4 Time-dependence of the SAXS invariant, Q' (□), and WAXS degree of crystallinity, X_C (●), during the melting and isothermal (133°C) recrystallization of iPP. The uncorrected temperature programme is indicated at the top of the figure

930 kg m^{-3} at 100°C and 850 kg m^{-3} at the melting point[27]. Solving the quadratic for Q' gives two sets of solutions for values of ϕ, which may be compared with the volume fraction calculated from A_C, so that only the most reasonable values are taken.

The values of ϕ are calculated from the WAXS data using the expression

$$\phi(\text{WAXS}) = I - I_a/2(I_{Q^*} - I_a) \qquad (8)$$

and values of ϕ, calculated from the quadratic equation of the invariant, after correction of the linear change in the (electron) density difference[23,24], are plotted against time in *Figure 6*. The correlation between the degree of crystallinity from WAXS and that from SAXS is good considering the assumptions made in the calculation.

In the two-phase model, the average lamellar thickness, L_C, is given by the product of the degree of crystallinity, ϕ, and the long spacing, d_1. *Figure 6* is a plot of the measured parameters, X and d_1, and the values of L_C calculated according to the two-phase model[3,10]. The degree of crystallinity decreases and the long spacing increases with temperature as expected; individual

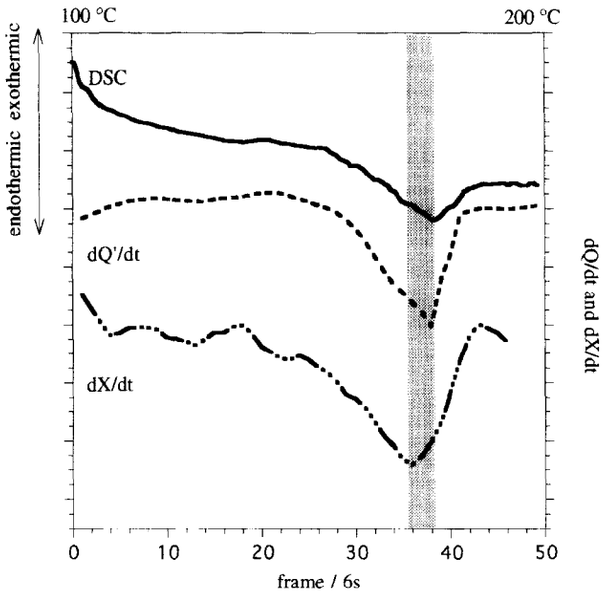

Figure 5 The differential with respect to time of the relative invariant, dQ'/dt (- - -), and the integrated WAXS intensities, dX/dt (— - - -), compared with the d.s.c. curve (——), obtained during the melting of iPP. The uncorrected heating programme (20°C min^{-1}) is indicated at the top of the figure. The shaded area, representing a 5°C temperature interval, encompasses the minima (at 170 ± 2°C) in the three curves. Exact correlation is obtained between d.s.c. and dQ'/dt data; correlation with dX/dt is less precise due to the intrinsic noise

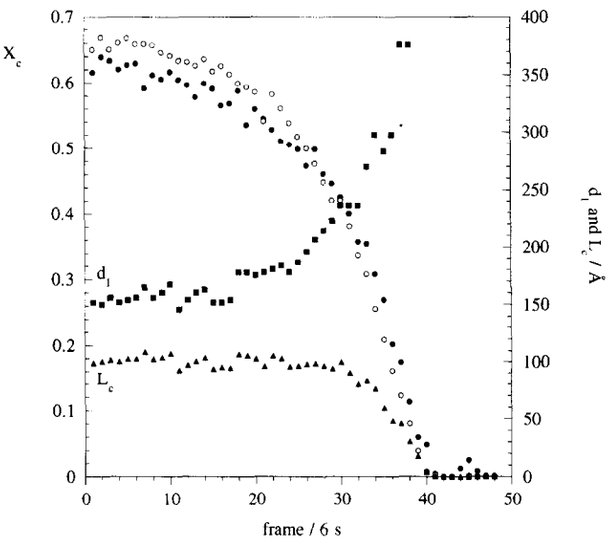

Figure 6 Variation with time of lamellar thickness, L_C (▲), long spacing, d_l (■), and degree of crystallinity, X_C (from WAXS ●, from SAXS ○), during the melting of iPP. The data have been derived on the basis of a simple two-phase model

lamellae melt in a first-order fashion, with the lower-order lamellae melting at lower temperatures. The average lamellar thickness remains constant and then decreases asymptotically at the melting point. This is counter-intuitive as the thinnest lamellae (those having the greatest fold surface area) should melt first causing the d-spacing to increase[3,6,7]. The experimental result may be rationalized, however, by considering a growing interface that causes an apparent reduction in ϕ.

The most generally used method of calculation of the lamellar thickness, multiplying the long spacing by the degree of crystallinity, is fundamentally in error unless $X_S = 1$. The SAXS invariant and WAXS intensities integrate over the whole of the sample whereas the degree of crystallinity required for the calculation of the lamellar thickness is that locally within the lamellar stacks. The correlation function, $\gamma_1(r)$, effectively ignores material not contained in lamellar stacks, and thus the regions of amorphous material remaining after melting of secondary crystallites are not included when calculating the linear crystallinity.

Figure 7a compares plots of $\log I(q)$ and the Lorentz-corrected intensities, $I(q)q^2$ vs q. The noise in the plots is just about within the limit that allows the correlation function programme to give reproducible results. The $\log I(q)$ data show the Guinier and damped Porod extrapolations. The data shown comprise one frame (115°C) taken with a time resolution of 6 s. The peak in the $I(q)q^2$ vs q curve is characteristic of the lamellar

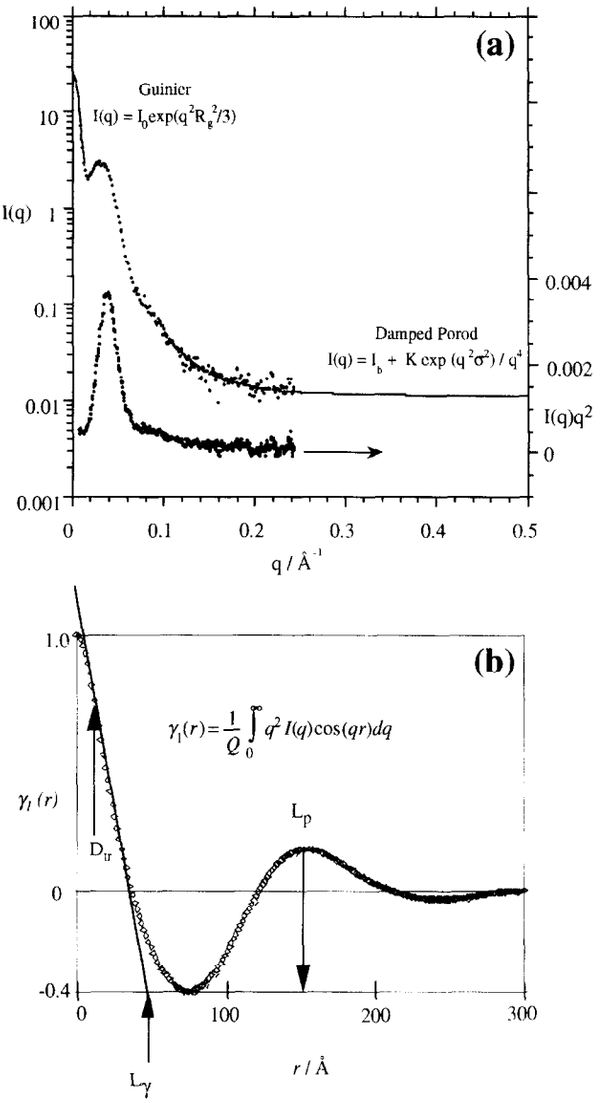

Figure 7 (a) A SAXS pattern (6 s of data collection) for iPP at ≈ 115°C. The upper curve is plotted as $\log I(q)$ vs q and illustrates the Guinier and damped Porod extrapolations (at low and high q, respectively), used to calculate the correlation function. The lower curve is $Iq^2(q)$ vs q and shows the peak used to calculate q^* by fitting a Gaussian function to the peak. (b) The correlation function, $\gamma_1(r)$ vs r, derived from the scattering pattern in (a), with the values of L_γ, L_p and D_{tr} as indicated

structure of the iPP, and the peak location ($q = 0.04\,\text{Å}^{-1}$) corresponds to a value of $d_1 = 157 \pm 3$ Å. There is also a weak second-order reflection centered around $q = 0.08\,\text{Å}^{-1}$.

The correlation function, $\gamma_1(r)$, plotted against r in *Figure 7b*, shows some noteworthy features. The function is smooth with insignificant noise, since each datum point contains all the information in the whole scattering curve. There are no fluctuations in the function introduced by joining the extrapolated data to the experimental data. Also, as r tends to zero, the gradient of the curve tends to zero indicating a good tail-fit of the data. If there were any errors in the extrapolations then these would be apparent as oscillations in the data where the join occurred (≈ 10 Å) and the slope at $r = 0$ would be steep. The interfacial thickness, D_{tr}, the length, L_γ, of the shortest stack, and the long period, L_p, may be obtained from $\gamma_1(r)$, as indicated in *Figure 7b*. Although values of length scales and degrees of crystallinity can be obtained from $\gamma_1(r)$, Babinet's principle applies and some *a priori* knowledge of whether the sample is more or less than 50% crystalline is required in order to calculate the thicknesses of the crystalline and amorphous regions[6]. The value of 153 Å for the long period, determined from $\gamma_1(r)$, is in good agreement with that, 157 ± 3 Å, calculated from Bragg's law. The analyses of the SAXS and WAXS data above, and of the off-line d.s.c. measurements of the enthalpy of fusion, provide the *a priori* information, so enabling the calculation of lamellar thickness and the thickness of the amorphous layer to be made: the values obtained are 109 and 44 Å, respectively. These data are used to give a linear degree of crystallinity of 0.71 which, as expected, is higher than X_C ($= 0.65 \pm 0.05$) as there is some amorphous material which is included in the X_C calculation but excluded from $\gamma_1(r)$. The value of the interfacial thickness is very sensitive to the tail-fit and has a random error of 3 Å. Nevertheless, the interfacial thickness increases systematically during melting and is constant during crystallization, and a value of 10 ± 3 Å, representing ≈ 5 monomer units, is reasonable for the transition zone from the crystalline region, with density 950 kg m^{-3}, to the amorphous region, with density 850 kg m^{-3}[27].

Comparative values of the degree of crystallinity, the long spacing and the lamellar thickness, calculated from the correlation function and the integrated intensities plus the invariant, are plotted as functions of time during the heating stage as shown in *Figure 8*. The most obvious feature is that d_γ maps onto d_1 throughout the melting process, validating the applicability of the 1-D correlation function. There are obvious differences between the values of X_γ and X_C, and between those of L_γ and L_C. These differences are of course related and are due to the integrated intensities, which include all the material, and the correlation function which analyses only that fraction of the sample that has a regular lamellar morphology.

As the material which crystallizes during secondary crystallization melts, either between lamellar stacks within a spherulite or between spherulites[23], the global degree of crystallinity, X_C, decreases whereas the local degree of crystallinity, X_γ, stays approximately constant. The lamellar thickness, L_γ, from the correlation function relates only to the material in lamellar stacks and there is an increase in the average lamellar thickness as the thinner lamellae melt. The lamellar thickness calculated from the integrated intensities is insensitive to the subtleties of the melting process and the average lamellar thickness is predicted to be constant, which is intuitively incorrect.

During primary crystallization, the detailed molecular structure of the polymer, the specific nature of the nucleation process and the degree of under-cooling determine the magnitude of the lamellar thickness and the degree of crystallinity within the lamellar stacks. The crystallization kinetics are analysed using the Avrami model[3,12], expressed in terms of the equation

$$1 - X_S = e^{kt^n} \tag{9}$$

where k is a rate constant and n is an integer interpretable in terms of the crystallization mechanism. *Figure 9* shows a plot of X_S vs t in which the experimental data have been fitted with the Avrami expression over the whole of the primary crystallization process. The fit to the data gives a value for the exponent, n, of 3.0 ± 0.1, with a precision of 4%. The value (3.0) obtained is consistent with random

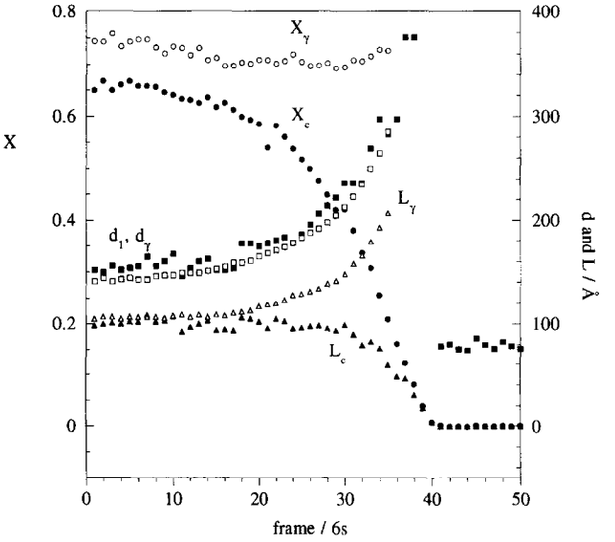

Figure 8 Comparison of the crystallinity, long spacing and lamellar thickness data obtained by the integrated intensities (closed symbols) and correlation function (open symbols) methods. The data were obtained simultaneously during the melting of iPP

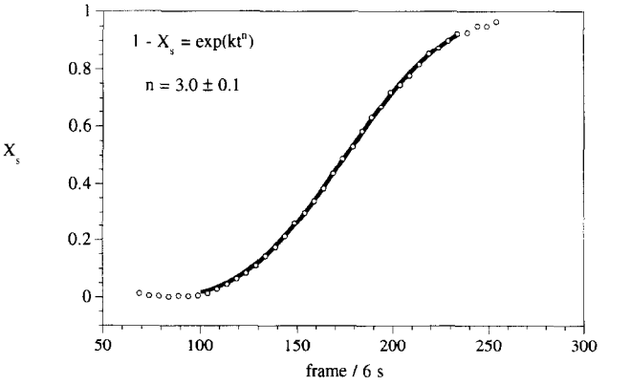

Figure 9 Variation with time of the volume fraction (X_S) of spherulites formed during the isothermal (133°C) crystallization of iPP. For clarity, only every tenth datum point is shown, and the solid curve is the fit to the data obtained using the Avrami expression with the value of the exponent, n, given in the inset

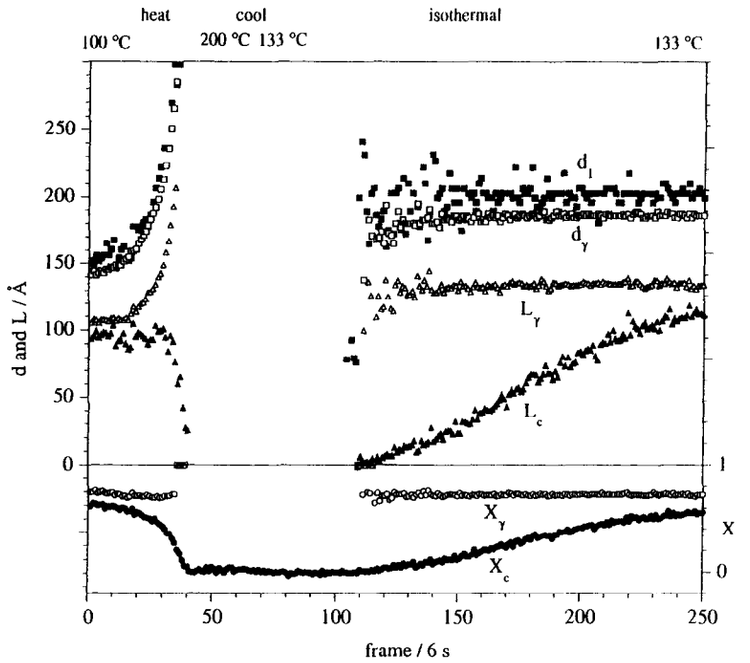

Figure 10 Combined melting and isothermal (133°C) crystallization behaviour of iPP, showing comparative plots of crystallinity, long spacing and lamellar thickness *versus* time. Data have been obtained by the integrated intensities (closed symbols) and correlation function (open symbols) methods. The erroneous nature of the data for the lamellar thickness (by the integrated intensities method) and the degree of crystallinity (by the correlation function method) should be noted

nucleation of spherulites, and is in good agreement with the crystallization kinetics data obtained from dilatometric and calorimetric studies on iPP[1].

In order to calculate the degree of crystallinity and the lamellar thickness during crystallization, a combination of both the integrated intensities and the correlation function is needed. The long spacings (d_γ and d_l) are constant during the growth process and, as $X_C(\propto X_S) \rightarrow 1$, there is a significant difference between $X_\gamma(\approx 0.65)$ and X_C. These data are shown in *Figure 10*. Both X_γ and L_γ are, in fact, constants during the growth process, and the changes in L_C are artefacts of the calculation. The true values for crystallization kinetics and the crystal size are obtained, respectively, from the integrated intensities and the correlation function.

SUMMARY AND CONCLUSIONS

The new SAXS/WAXS/d.s.c. at the SRS has been used to follow the recrystallization and melting of iPP. The agreement in the location of transitions between the differentials, with respect to time (which is equivalent to temperature), of the invariant and integrated WAXS intensities, and of the d.s.c.-curve, was shown to be within the time-resolution of the instrument.

The degree of crystallinity and lamellar thickness of iPP have been calculated from SAXS and WAXS patterns, obtained simultaneously during melting and crystallization, by integrated intensity and correlation function techniques. The long spacing was obtained from the peak in Lorentz-corrected SAXS pattern and was in good agreement with that calculated from the correlation function. The degree of crystallinity was obtained by a combination of the SAXS invariant and the integrated WAXS intensity due to the crystals, and the local crystallinity was obtained from $\gamma_1(r)$. The melting process was characterized by a gradual reduction in the degree of crystallinity and an increase in the long spacing, at a constant local crystallinity, due to first-order melting of low-order crystals. These two effects, when combined, gave a lamellar spacing (from the integrated intensity method) that did not appear to change during the melting process, which is counter-intuitive[7,24], whereas the lamellar thickness from $\gamma_1(r)$ increased during the melting process which is consistent with the initial melting of thin lamellae.

During the isothermal crystallization process the same phenomena were observed, in the SAXS and WAXS data analysed by the integrated intensities and the correlation function, as for the melting process, and their interpretation was identical: the local crystallinity and lamellar thickness from $\gamma_1(r)$ were constant during growth characterizing the crystalline structure whereas the integrated intensities characterized the growth of spherulites as $X_C \propto X_S$, and X_S tends to unity. Future work will concentrate on the crystallization of polymer in the presence of fillers and nucleating agents. Crystallization during extrusion is also being studied. The methodologies developed here will be used to extract crystallization rates and crystal structure directly from the X-ray data.

ACKNOWLEDGEMENTS

The authors thank EPSRC for beam-time at Daresbury and provision of funding under grant GR J24713. Beamline 8.2 was built under an agreement between the Daresbury Laboratory and the Netherlands Organisation for Scientific Research (NWO). Thanks are also due to Rob Rule, ICI, for helpful discussions and to Bryan Wood, Manchester Materials Science Centre for preparing the iPP samples. Collaboration with Cabot Plastics, Dukinfield, Cheshire, UK is acknowledged.

REFERENCES

1 Karker-Kocsis, J. (Ed.) 'Polypropylene', Vol. 1, Chapman & Hall, London, 1995
2 O'Kane, W. J., Young, R. J. and Ryan, A. J. *Macromol. Sci.-Phys.* 1995, **B34,** 427
3 Sperling, L. H. 'Introduction to Physical Polymer Science', John Wiley & Sons, New York, 1986
4 Immergut, E. (Ed.) 'Polymer Handbook', John Wiley & Sons, New York, 1989
5 Tsuji, M. 'Comprehensive Polymer Science' (Eds G. Allen and G. C. Bevington), Vol. 1, Pergamon Press, Oxford, 1988, Ch. 34, p. 785
6 Baltá-Calleja, F. J. and Vonk, C. G. 'X-ray Scattering of Polymers', Elsevier, Amsterdam, 1989
7 Ruland, W. *Acta Cryst.* 1961, **14,** 1180
8 (a) Ullmann, W. and Wendorff, J. H. *Prog. Coll Polym. Sci.* 1979, **6,** 25; (b) Cheng, S. Z., Janimak, J. J. and Zhang, A. *Polymer* 1991, **32,** 648; (c) Bu, H. S., Cheng, Z. S. D. and Wunderlich, B. M. *Makromol. Chem. Rapid Commun.* 1988, **9,** 76
9 Vonk, C. G. *J. Appl. Cryst.* 1975, **8,** 340
10 Strobl, G. R. and Schnieder, M. J. *J. Polym. Sci., Polym. Phys. Ed.* 1981, **19,** 1361
11 Ruland, W. *J. Appl. Cryst.* 1971, **4,** 70
12 Marker, L., Hay, F. M. and Tilley, G. P. *J. Polym. Sci.* 1959, **38,** 107
13 Nakamura, N. K. *J. Appl. Polym. Sci.* 1973, **17,** 1031
14 Magill, J. H. *Polymer* 1962, **3,** 35
15 Schoeterden, P., Vandermarliere, M., Reikel, C., Koch, M. H. J., Groeninckx, G. and Reynaers, H. *Macromolecules* 1989, **22,** 237
16 O'Kane, W., Ryan, A. J., Young, R. J., Bras, W., Mant, G. R. and Derbyshire, G. E. *Polymer* 1994, **35,** 1353
17 Burke, M., Stanford, J. L. and Young, R. J. *Plast. Rubb. Comps. Proc. Appl.* 1993, **20,** 121
18 Wood, B. M. and Stanford, J. L. Unpublished work, 1993
19 Bras, W., Derbyshire, G. E., Ryan, A. J., Mant, G. R., Felton, A., Lewis, R. A., Hall, C. J. and Greaves, G. N. *Nucl. Instrum. Meth. Phys. Res.* 1993, **A326,** 587
20 Ryan, A. J. *J. Therm. Anal.* 1993, **40,** 887
21 Bras, W., Derbyshire, G. E., Mant, G. R., Clarke, S. M., Cooke, J., Komanschek, B. U. and Ryan, A. J. *J. Appl. Cryst.* 1994, **28,** 26
22 Ryan, A. J., Komanschek, B. U., Naylor, S., Bras, W., Mant, G. R. and Derbyshire, G. E. *ACS Symp. Ser.* 1994, **581,** 162
23 Bark, M. and Zachmann, H. G. *Acta Polym.* 1993, **44,** 259
24 Ryan, A. J., Bras, W., Mant, G. and Derbyshire, G. *Polymer* 1994, **35,** 4537
25 Ryan, A. J., Willkomm, W. R., Bergstrom, T., Macosko, C. W., Koberstein, J. T., Yu, C. C. and Russell, T. P. *Macromolecules* 1991, **24,** 2883
26 The degree of crystallinity after complete crystallization at $T = 133°C$ is never as high as that in a sample which has been cooled to room temperature and undergone secondary crystallization.
27 van Krevelen, D. W. 'Properties of Polymers: Correlations with Chemical Structure', 3rd Edn, Elsevier, Amsterdam, 1991